

Article citation info:

Capała P, Ruzsak M, Czyż Z, Rudawska A, Comparative analysis of different catalytic baskets for dual-bed catalytic reactors, *Eksploracja i Niezawodność – Maintenance and Reliability* 2025: 27(3) <http://doi.org/10.17531/ein/200290>

## Comparative analysis of different catalytic baskets for dual-bed catalytic reactors

Indexed by:



Paweł Capała<sup>a,b,\*</sup>, Monika Ruzsak<sup>a</sup>, Zbigniew Czyż<sup>c</sup>, Anna Rudawska<sup>b</sup>

<sup>a</sup> Nitric Acid Technology Department, Łukasiewicz Research Network—New Chemical Syntheses Institute, Poland

<sup>b</sup> Faculty of Mechanical Engineering, Lublin University of Technology, Poland

<sup>c</sup> Faculty of Aviation, Polish Air Force University, Poland

### Highlights

- The structure of different catalytic baskets for dual bed reactors was discussed.
- The contours of linear velocity in the catalyst beds were assessed.
- The contours of pressure drop in the catalyst beds were assessed.
- The linear velocity and pressure drop results were analysed and assessed in the dual beds.

### Abstract

Catalytic baskets used to support catalyst beds can have different designs. For industrial practice, reactors with axial and radial gas flow direction through the catalyst bed are commonly used. The influence of the tail gas distribution in a dual-bed catalytic reactor on the linear gas flow velocity and pressure drop across the catalyst bed was analysed. The analyses were performed for the reactor's use in a pilot nitric acid plant for axial-radial and radial catalytic basket designs. The results indicated a significant influence of the basket design on the linear gas flow velocity profile and pressure drop distribution in a dual-bed catalytic reactor. The most advantageous solution was the coaxial arrangement of the catalyst beds without separating them with a space, which can affect the reliability of the reactor. The lowest linear flow velocity and gas flow resistance values in a dual-bed catalytic reactor were obtained for the mixed axial and radial gas flow through the catalysts beds, separated only with a porous baffle.

### Keywords

catalysts beds, dual bed reactor, catalytic basket design, purifying the tail gas, reliability catalytic reactor, NO<sub>x</sub> and N<sub>2</sub>O.

This is an open access article under the CC BY license (<https://creativecommons.org/licenses/by/4.0/>)

### 1. Introduction

Industrial plants, carrying out processes of burning fossil fuels (e.g. heat and power plants) or ammonia oxidation (e.g. nitric acid and caprolactam plants), are a source of nitrogen oxides NO<sub>x</sub> and N<sub>2</sub>O emissions into the atmosphere. N<sub>2</sub>O is a potent greenhouse gas with a GWP index 265-298 times greater than CO<sub>2</sub> (GWP = 273 over a 100-year time horizon) [1]. Nitrogen oxides are indirect greenhouse gases [2]. The need to limit their emissions into the atmosphere is primarily due to their harmful impact on human health and the environment [3,4,5]. The

limitation value of NO<sub>x</sub> is regulated by law by the Directive 2010/75/EU, while their levels are set by the Council's Decision (EU) 2017/1757 of 17 July 2017 *on the acceptance on behalf of the European Union of an Amendment to the 1999 Protocol to the 1979 Convention on Long-Range Transboundary Air Pollution to Abate Acidification, Eutrophication and Ground-Level Ozone*, as well as the BAT Reference Document [6]. N<sub>2</sub>O emission standards are still being tightened, which is associated with the pursuit of achieving "climate neutrality" in 2050.

(\*) Corresponding author.  
E-mail addresses:

P. Capała (ORCID: 0000-0002-7574-9433) [pawel.capala@ins.lukasiewicz.gov.pl](mailto:pawel.capala@ins.lukasiewicz.gov.pl), M. Ruzsak (ORCID: 0000-0002-7883-7439) [monika.ruzsak@ins.lukasiewicz.gov.pl](mailto:monika.ruzsak@ins.lukasiewicz.gov.pl), Z. Czyż (ORCID: 0000-0003-2281-1149) [z.czyz@law.mil.pl](mailto:z.czyz@law.mil.pl), A. Rudawska (ORCID: 0000-0003-3592-8047) [a.rudawska@pollub.pl](mailto:a.rudawska@pollub.pl),

Currently, the descent of  $N_2O$  to a greater extent beyond the applicable limitations is associated with financial benefits of around 80 EUR for each additionally reduced one ppm of nitrous oxide [7].  $NO_x$  emission standards may soon be tightened. In nitric acid plants, achieving the current  $NO_x$  emission limits requires using a high-efficiency absorption or SCR-de $NO_x$  technology [8]. Due to the legal and economic aspects mentioned, it is necessary to seek effective and reliable solutions to reduce  $NO_x$  and  $N_2O$  emissions. Currently, the best available techniques for descending emission in industrial plants are the Selective Catalytic Reduction of  $NO_x$  (SCR-de $NO_x$ ) and  $N_2O$  (SCR-de $N_2O$ ) and low-temperature catalytic decomposition of nitrous oxide (LT-de $N_2O$ ). Maintenance of the SCR-de $NO_x$  and de $N_2O$  processes in one reactor is a beneficial solution, as it ensures lower capital and operating costs for tail gas purification. The beds of both catalysts can contact each other through a porous wall or can be spatially separated. The space between the beds is usually the injection zone of the reducing agent (for  $NO_x$  or  $N_2O$  reduction) before the second catalytic layer [9-12]. The performance and reliability of a catalytic process are influenced not only by the catalyst composition and shape but also by the configuration of the bed in the catalytic basket. Baskets used to support de $NO_x$  and de $N_2O$  catalyst beds can have different designs, while the most commonly used solutions are those forcing the axial and radial direction of the purified gas flow through the beds. Modifying this design allows one to influence the way the gas is distributed on the catalysts beds, the pressure drop, and the linear gas flow velocity. If an SCR-de $NO_x$ /de $N_2O$  reactor is installed before the expansion turbine, the lowest possible gas pressure drops in the reactor must be ensured to achieve the highest possible energy recovery in the expansion turbine (lower operating costs). Gas flow resistance is directly related to the linear gas flow velocity, influencing the catalytic reaction rate in the diffusion regime. Our experience shows that descending the gas velocity value in the formed catalytic layer reduces the gas resistances across the catalytic zone and increases the efficiency and reliability of the SCR-de $NO_x$ /de $N_2O$  technology [13-16].

Experimental verification of the SCR-de $NO_x$ /de $N_2O$  technology enables the evaluation of its efficiency (by determining the catalyst selectivity, the degree of  $NO_x$  and  $N_2O$  reduction or  $N_2O$  decomposition), determination of the linear

velocity and the flow resistances through the bed. However, measuring parameters inside the catalysts beds is difficult. In this case, computational fluid dynamics software (CFD) is a helpful tool. It allows one to understand the hydrodynamics of gas flow throughout the structured and unstructured catalysts beds for different flow geometries and to analyse the effect of disturbances (static mixers, solid and perforated baffles, porous bodies) on the flow parameters. The CFD method is an important work tool for engineers. It allows for quick verification of proposed design solutions without creating further cost-consuming reactor prototypes and enables the optimisation of these solutions. It accurately reflects the fluid's behaviour in a given medium/reactor, provided that an appropriate geometry is defined for the considered computational domain, and this domain is well discretized into small volumes or elements in which partial differential equations are solved [17-26]. Many scientific studies on CFD modelling of SCR-de $NO_x$  reactors, intended for heat and power plants, mainly focus on analysing the gas flow field in the reactor space upstream of the catalyst bed. They concern the influence of the change of the flow cross-sectional area and the presence of baffles and static mixers on the distribution of the linear gas flow velocity and the reactant concentration profile. Few studies analyse the gas flow velocity and resistance distribution in the catalyst bed, especially in SCR-de $NO_x$ /de $N_2O$  reactors used in nitric acid or caprolactam plants (end-of-pipe SCR reactors). The greater need to understand the flow mechanics in SCR reactors used in heat and power plants results from several aspects:

- they are several times larger than those used in nitric acid or caprolactam plants, so it is difficult to obtain a uniform flow distribution inside the reactor,
- gas flow rates are much higher, so it is essential to ensure the lowest possible gas flow resistances.

The ammonia injection zone is located inside the reactor. To obtain higher efficiency and reliability of SCR-de $NO_x$  technology is crucial to ensure a uniform distribution of ammonia in the purified gas stream (a uniform  $NH_3/NO$  concentration profile) [27-31].

Vandewalle et al. analysed the hydrodynamics of a gas flow inside the catalyst bed using the example of a lateral reactor, which can be used in the end-of-pipe SCR-de $NO_x$  technology in

nitric acid and caprolactam plants. The influence of bed packing, reactor geometry, and operating parameters on the distribution of pressure drops and linear gas flow velocities inside the catalyst bed was analysed. The authors emphasized the significant influence of pressure drop gradients upstream of the catalyst slabs on the gas distribution inside these slabs in the axial direction and the efficiency of the SCR-deNO<sub>x</sub> technology (to obtain >95% NO<sub>x</sub> conversion it was necessary to ensure flow homogeneity in the axial direction at the level of >50%). Lateral and radial reactors, as well as those containing monolithic catalysts, are industrial reactors that provide low-pressure drops through the catalytic bed [32]. There is no similar analysis of the gas flow hydrodynamics in other types of SCR-deNO<sub>x</sub> and/or deN<sub>2</sub>O reactors, especially considering the influence of the basket design on the pressure drops and linear gas flow velocities distribution in the area of the catalysts beds.

This paper presents the results of CFD modelling for the catalytic reactor used in the pilot nitric acid plant of Łukasiewicz—INS. It is designed to purify the tail gases stream from nitrogen oxides NO<sub>x</sub> and/or N<sub>2</sub>O through the catalyst bed. Based on this reactor, a computational domain was built to analyse the influence of different catalytic basket designs on the hydrodynamics of gas flow in a dual-bed catalytic system. This type of solution can be used when two catalytic processes, e.g., SCR-deNO<sub>x</sub> and LT-deN<sub>2</sub>O, are carried out in one reactor in the presence of two catalysts beds. Understanding the local flow dynamics in dual-bed catalyst models improves the performance of SCR-deNO<sub>x</sub>, deN<sub>2</sub>O, and other catalytic processes. However, comprehensive research has not been conducted so far. Based on CFD simulations, the influence of the mutual arrangement of catalysts beds and the way of realizing the gas flow through these beds (gas flow in the radial or axial direction) on the pressure drops and linear gas flow velocities distribution inside the catalytic reactor was analysed. If internal reaction rates are high, this negatively affects catalytic processes. The same reactor operating parameters and boundary conditions were assumed for each case. The design solutions for the catalytic baskets presented in this work are intended to install the beds of the shaped catalyst bodies (tablets, extrudates, spheres and others). Therefore, the bed was modelled as a porous medium to simplify the simulation process [27,33].

## 2. Computational method

### 2.1. The geometry of a dual-bed catalytic system and computational domains

The computational domains are based on the geometry of the real SCR-deNO<sub>x</sub>/LT-deN<sub>2</sub>O reactor, one of the technological nodes of the Łukasiewicz - INS pilot nitric acid plant. It is designed for catalytic purification of the gases from NO<sub>x</sub> and N<sub>2</sub>O. A basket with a catalyst bed can have a different construction, forcing different directions of purified gas flow throughout the catalytic zone. Four design solutions of the catalytic baskets, placed inside the domain representing the pilot reactor geometry, were modelled using CFD method. They corresponded to different ways of arranging two catalysts beds relative to each other and various directions of the gas flow throughout these beds: axial-radial and radial.

Fig. 1 shows the pilot catalytic reactor, based on which the computational domains were built. Its dimensions, defined by diameter and height, are 400 x 700 mm. Inside the reactor, a catalytic basket with maximum dimensions of d x h = 300 x 400 mm, can be installed.



Fig. 1. The SCR-deNO<sub>x</sub>/LT-deN<sub>2</sub>O reactor, constituting one of the technological nodes of the pilot nitric acid plant, on which the geometry of the computational domain was based.

The models of the catalytic reactor with different basket designs, used to build the computational domains, were designated as follows:

- Model 1 – axial-radial flow reactor with two catalysts beds arranged one above the other, separated from each other by a space along the axial direction;
- Model 2 – radial flow reactor with two catalysts beds, arranged one above the other, separated from each other by a space along the axial direction [9];
- Model 3 – radial-axial reactor with two catalysts beds arranged coaxially along the reactor diameter, separated by porous baffles, perpendicular and parallel

to the reactor axis [34];

- Model 4 - radial reactor with two catalyst beds, separated by a porous baffle [10].

The models do not include support elements, flat bars, or others, not affecting the gas flow through the catalysts beds. Only a deflector in the reactor inlet and outlet zone was considered to increase the gas flow stability and better gas distribution in the catalyst bed. Deflectors are often installed in zones, where the reactor's flow cross-section changes.

Fig. 2 shows methods of arranging two catalysts beds in a pilot reactor, based on which computational domains were built.

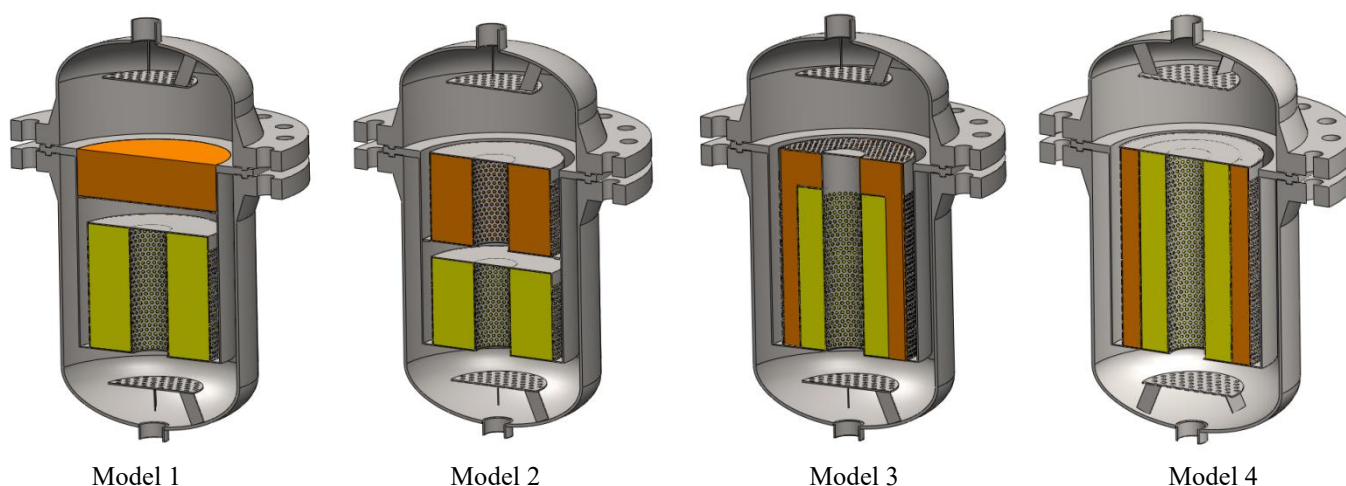


Fig. 2. Geometric models of the pilot reactor interior with a dual-bed catalytic system, differing in gas flow through the catalysts beds and their mutual arrangement.

Table 1 Structural parameters of SCR-deNO<sub>x</sub>/LT-deN<sub>2</sub>O pilot reactor.

Dual-bed catalytic reactor	Size
Reactor height, mm	750
Reactor diameter, mm	400
Reactor inlet size, mm x mm	50
Reactor outlet size, mm x mm	50
Thickness of catalyst layer (bed A), mm	Model 1: 96 Model 2: 96 Model 3 THK <sub>vertical</sub> : 73 THK <sub>lateral</sub> : 40 Model 4: 40
Thickness of catalyst layer (bed B), mm	Model 1: 96 Model 2: 96 Model 3: 56 Model 4: 56

Based on the above-mentioned geometric models of the pilot reactor, four computational domains were created in Catia V5.

These domains constitute a spatial representation of the reactor interior geometry (gas flow zone) with a dual-bed catalytic system. They differ in the way gas flows through the catalysts beds and their mutual arrangement. Each domain was assigned an identical global coordinate system and oriented in space in the same way. The domains were imported to Design Modeler, simplified, and divided into domains. The reactor is axisymmetric; therefore, to shorten the computational time, each domain was divided along the z-axis into four equal parts using two perpendicular cutting planes, as shown in Fig. 3. This allowed to limit the computational domain to a "quarter model", from which the geometry of the entire reactor interior can be recreated through symmetry operations (reflections in the plane).

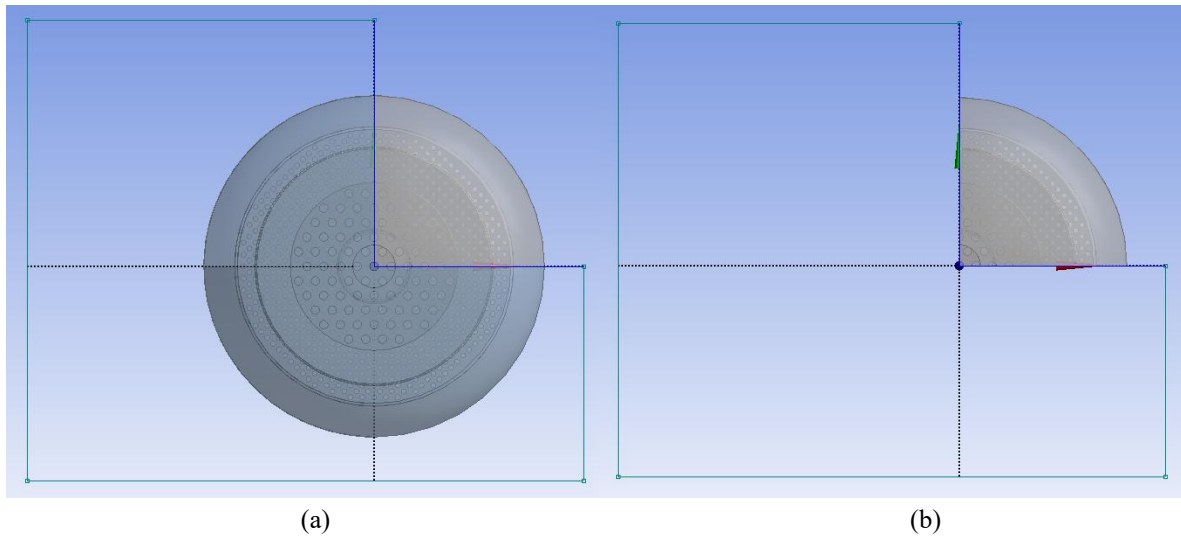


Fig. 3. Division of the computational domain into four identical parts (a) – separation of the “quarter model” for numerical calculations (b).

In the next step, the domain was divided into four domains, representing different areas inside the reactor (Fig. 4):

- inlet section – extending from the reactor inlet to the first catalytic section (bed A),
- first catalytic section (catalyst bed A) – modelled as a porous medium,
- second catalytic section (catalyst bed B) – modelled as a porous medium,

- outlet section including the central perforated pipe along the reactor axis and the space between the second catalytic section and the reactor outlet.

In Models 1 and 2, an additional section between the catalyst beds was created. Figure 4 shows four "quarter models" (quarter-domains), which serve as the final computational domains, along with the designated domains, representing four variants of the dual-bed catalytic reactor.

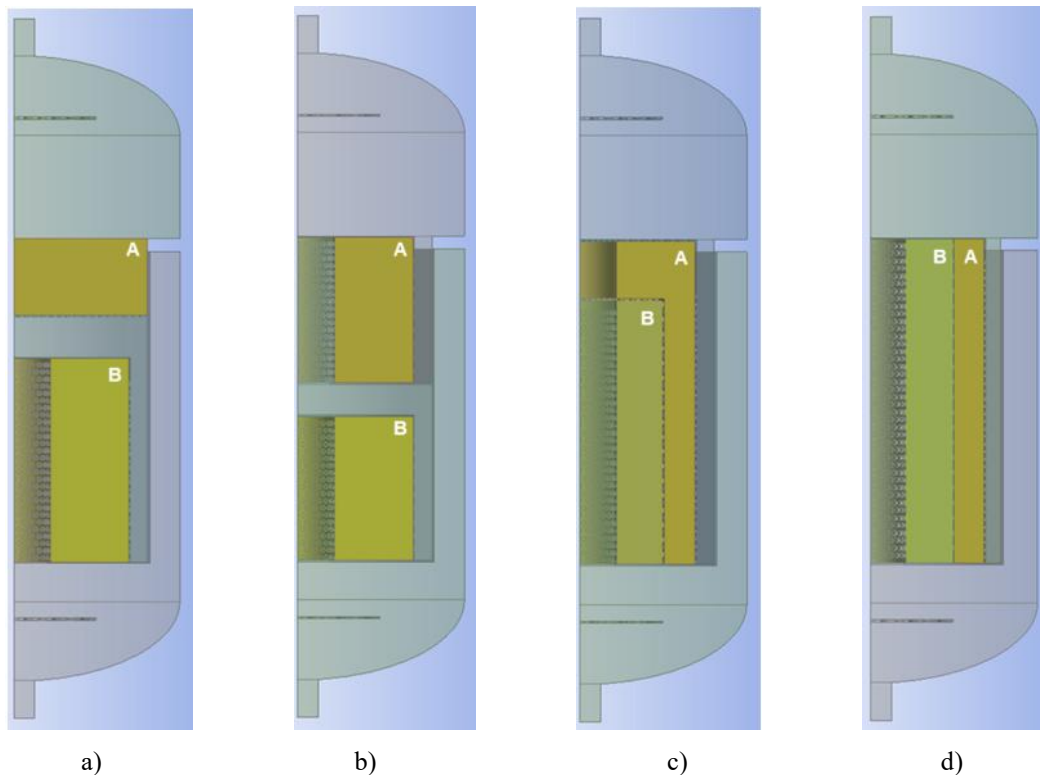


Fig. 4. Computational domains for four variants of the dual-bed catalytic reactor and designated domains for which CFD calculations were performed (A and B – catalytic sections with catalysts beds): a) Model 1, b) Model 2, c) Model 3, d) Model 4.

## 2.2. Discretisation of the computational domain

The computational domains were discretized in Ansys Meshing using the Tetrahedrons method with the Patch Conforming algorithm. An unstructured grid was used for each model, consisting of tetrahedral elements, with a maximum element/cell size of 4 mm and refined near the domain walls to 1 mm, with a growth factor of 1.2. A Boundary Layer at the boundaries of domains (shown in Fig. 5), consisting of 5 sublayers, was considered (a smooth transition between layers was ensured using the Smooth Transition Option algorithm). The number of mesh elements was determined by identifying the minimum mesh density, at which the results cease to change noticeably with further densification. For the initial (reference) model, several mesh variants with different densities were prepared, and calculations were performed on the same

boundary conditions. Comparing the key results regarding flow velocity and pressure drop, a mesh was selected for which the difference in results between successive densifications was negligible. By increasing the mesh density, attention was paid mainly to areas with significant changes in the recorded values. The number of mesh elements and nodes and the skewness coefficient values for the discretized computational domains are presented in Table 2:

Table 2. Computational grid parameters for the discretized computational domains, representing four variants of the dual-bed catalytic reactor.

Computational domain	Number of grid elements	Number of grid nodes	Coefficient of mesh skewness
Model 1	8,717,985	2,440,282	0.88689
Model 2	9,185,292	2,605,615	0.89630
Model 3	13,229,373	3,840,821	0.89816
Model 4	13,373,699	3,891,747	0.88786

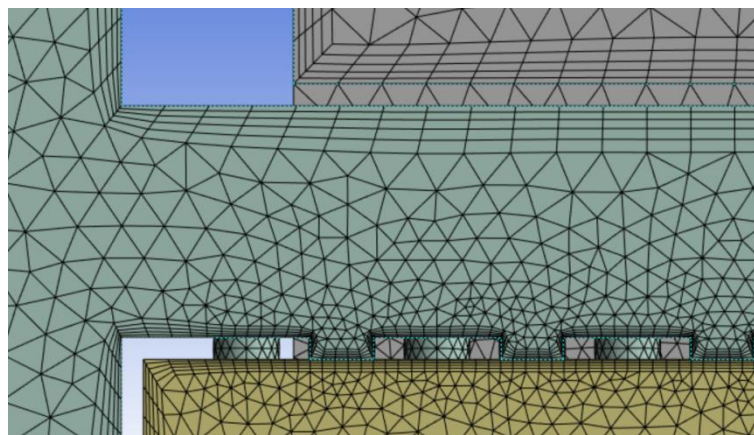
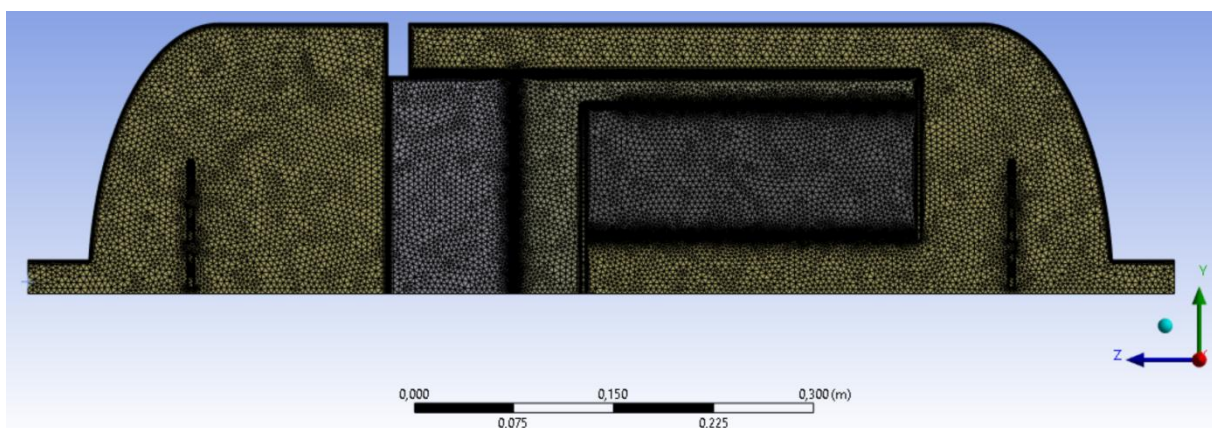


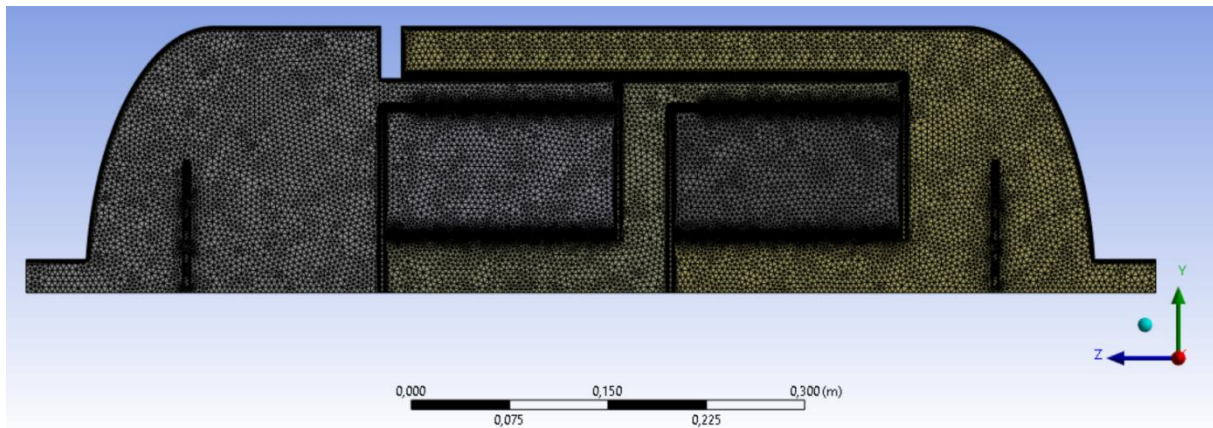
Fig. 5. A view of an example boundary layer at the boundary of domains.

The values of the grid skewness coefficients for individual domains are  $< 0.95$ , indicating a relatively good quality of the generated computational grid. The discretized computational

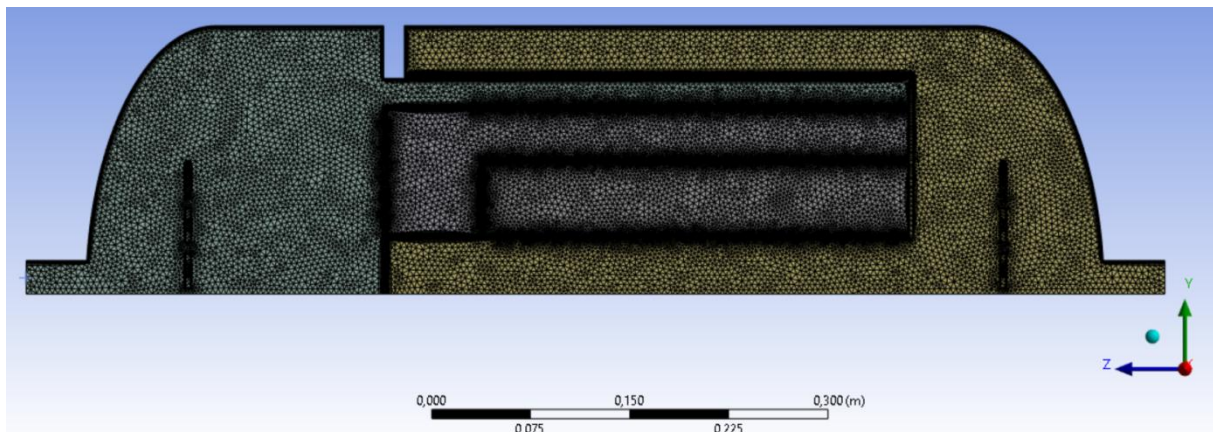
domains for the four variants of a dual-bed catalytic reactor are shown in Fig. 6.



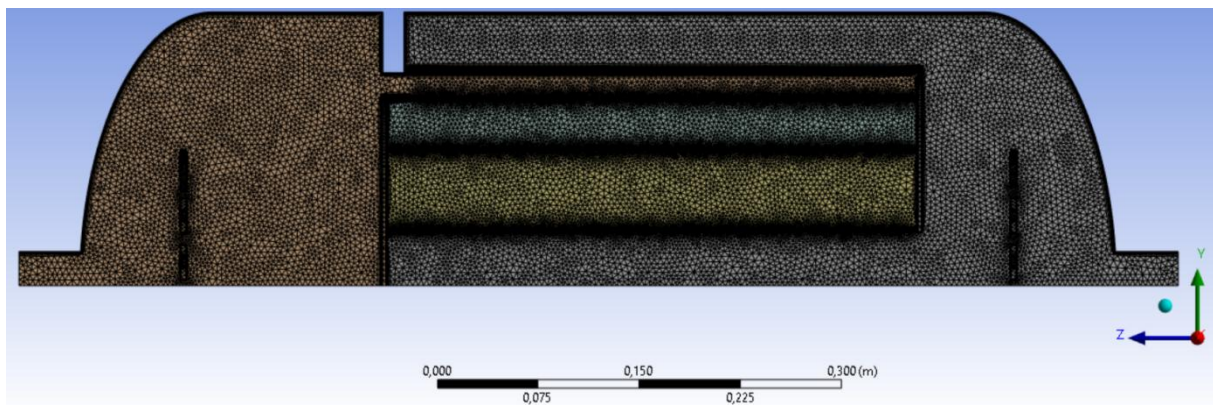
a)



b)



c)



d)

Fig. 6. Computational grids for individual variants of the dual-bed catalytic reactor: a) Model 1, b) Model 2, c) Model 3, d) Model 4.

### 2.3. Boundary conditions

The 3D flow was modelled by Ansys Fluent 2023 R2 software, which uses the subdomain method to discretise the differential equations. The  $k-\omega$  SST (shear stress transport) turbulence model was selected for numerical calculations. It introduces two additional transport equations into the system of averaged Navier-Stokes equations: one for turbulent kinetic energy and

one for its dissipation rate. This model accurately represents turbulence in the near-wall region, exhibits low sensitivity to boundary conditions for the inlet disturbances, and effectively images gas flow resistance through the packed layer of the catalyst. For numerical calculations, second-order differential equations were used to spatially discretise kinetic energy turbulence, turbulent dissipation rate, and energy equations.

For pressure and velocity coupling, the SIMPLE algorithm

was applied. The simulation results assessed convergent after achieving residual error values less than  $10^{-5}$  for all governing equations.

The pressure drop across catalyst beds is related to the linear gas flow velocity and bed porosity. Porosity ( $\epsilon$ ) is determined by the catalyst's particles size, shape and arrangement. In the case of randomly filled packed beds, which are the subject of this work, they were modelled as a porous medium. Experimentally verified the porosity of catalyst beds. The experiment obtained the graph of pressure drop versus working medium flow rate for the velocities corresponding to the ranges that occur in the catalyst beds. The experiment was made for the catalyst in the form of extrusions (2 mm in diameter and 2-6 mm in length) of a randomly filled packed bed, installed in the Łukasiewicz – INS pilot reactor. To define the porous medium, the viscous resistance  $1/\alpha$  [ $1/m^2$ ] and inertial resistance  $C_2$  [ $1/m$ ] were determined. In the function  $y=y(x)$  approximating the change in pressure drop, the slope coefficient A was 580.83, and the coefficient B was 509.87, respectively. Porous medium is defined by the parameters viscous resistance  $1/\alpha=B/(\mu \cdot n)$  and inertial resistance  $C_2=A/(\rho \cdot n)$  where:

$\mu$  - dynamic viscosity [ $Pa \cdot s$ ]

$n$  - thickness [ $m$ ]

$\rho$  - density [ $kg/m^3$ ]

The porous medium was defined by viscous resistance  $1/\alpha=1.626E+08$  [ $1/m^2$ ] and inertial resistance  $C_2 = 2.334E+04$  [ $1/m$ ].

Viscous resistance describes the resistance associated with the viscous friction of a fluid flowing through a porous medium. It accounts for the linear relationship between pressure losses and flow velocity (by Darcy's law). In contrast, inertial resistance describes the resistance resulting from the fluid's inertial effects, which become significant at higher flow velocities. It introduces a quadratic relationship between pressure losses and velocity.

In the next stage, the boundary conditions for the CFD calculations were determined:

- the computational domains had one gas inlet and one gas outlet,
- a uniform velocity profile at the inlet was assumed,
- a steady-state gas flow was assumed,
- the gas flow velocity at the inlet was set at 10.85 m/s,

- the gas outlet was set as pressure, assuming that the outlet pressure was the standard atmospheric one,
- the gas was modelled as air, and its parameters were determined for a temperature of 673K, density of  $0.524$   $kg/m^3$ , and viscosity of  $3.30 \times 10^{-5} Pa \cdot s$ ,
- the composition of the gas mixture was neglected,
- chemical reactions on the catalysts' surface were not taken into account,
- the density and viscosity of the gas were assumed to be constant,
- the symmetry boundary condition was applied on the cross-section surfaces of the quarter model,
- the porous zone parameters were assumed to be identical for the axial and radial directions,
- the catalysts beds were modelled as a porous medium,
- turbulence in the porous medium was suppressed (laminar zone).

The boundary conditions for numerical calculations were selected based on exemplary operating conditions of the SCR-deNO<sub>x</sub> reactor, one of the technological nodes of the Łukasiewicz - INS pilot nitric acid plant.

### 3. Discussion

CFD numerical calculations were performed to analyse the influence of the catalytic basket design, intended for installing two catalysts beds in one reactor, on the hydrodynamics of the purified gas flow in the catalytic zone. The pressure drop and gas velocity fields distributions were determined for the four variants of two catalysts beds arrangements (four catalytic basket models) inside the modelled reactor, which differed in the gas flow direction throughout beds A and B (axial-radial and radial) and their arrangement relative to each other (beds in contact through the porous baffles or spatially separated). The research aimed to find a design solution for a dual-bed catalytic reactor that ensured the lowest possible values of linear gas flow velocity and gas flow resistance through the bed. The velocity gas value in the bed influences the efficiency and reliability of the catalytic process running on the shaped catalysts beds. It ensures the correct catalytic reactions occur in the dynamic control flow. In nitric acid plants, low-pressure drops in the SCR-deNO<sub>x</sub>/deN<sub>2</sub>O reactor entail more energy recovery in the expansion turbine and lower operation costs. Low  $\Delta P$  values are

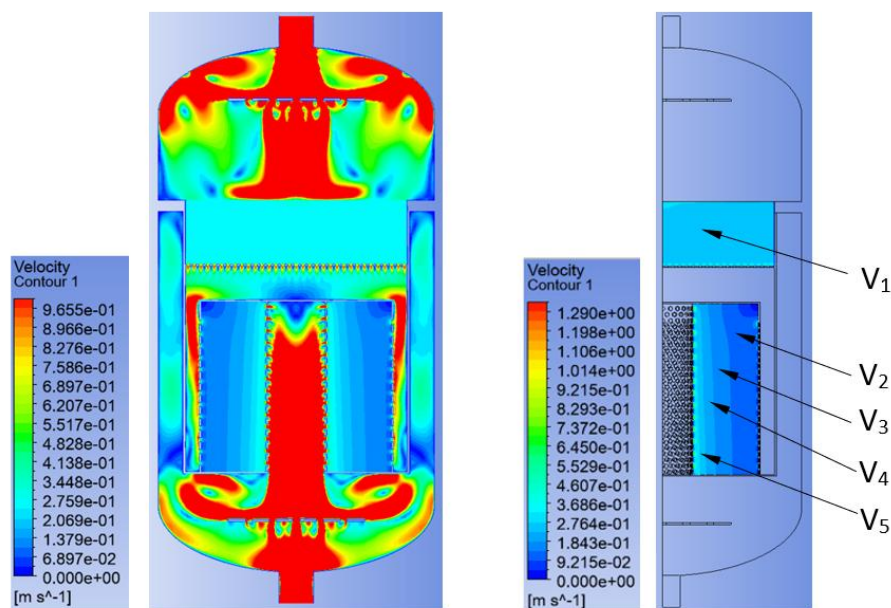
also desirable in the *end-of-pipe* SCR-deNO<sub>x</sub>/deN<sub>2</sub>O technology, to ensure a sufficient pressure value before the gas inlet to the stack.

### 3.1. Linear gas flow velocity profile

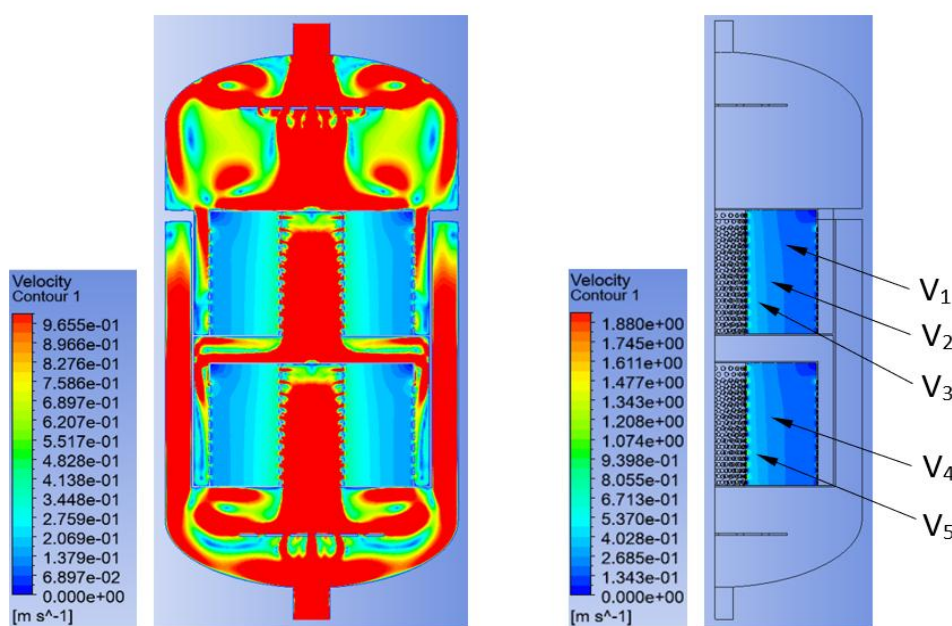
The contours of the fields of the velocity values inside the dual-bed catalytic model for the four variants of catalytic baskets designs are shown in Fig. 7. The domains on the right indicate the locations of linear velocity measurements inside the catalyst beds, representing fields of equal linear velocity.

Linear velocity measurements in fields where values were

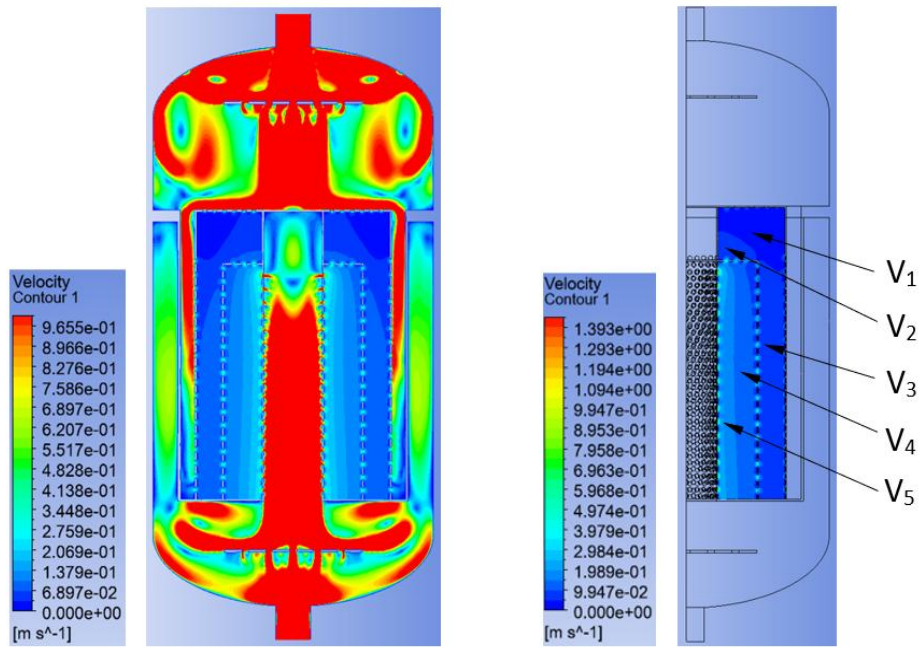
close to zero were omitted. These are the so-called dead zones formed near the solid impermeable cover and impermeable side walls in radial flow baskets. The results of these measurements are summarized in Table 3. In the analysed geometry of the computational domain, the cross-section of the gas flow field changes over a short section from the gas inlet through the space between the catalysts beds to the reactor outlet. Changing the way distribution and the profile of its flow field causes turbulence in the gas stream. Hence, the deflectors were used upstream and downstream of the catalytic sections.



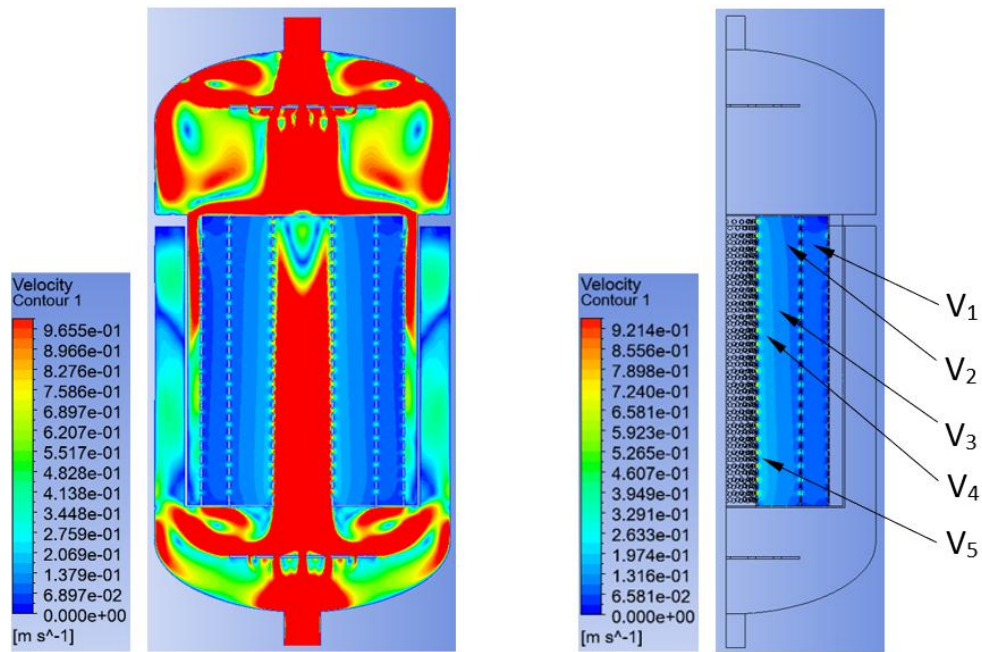
a)



b)



c)



d)

Fig. 7. Contours of the linear gas flow velocity fields inside the computational domains, representing different variants of the dual-bed catalytic reactor: a) Model 1, b) Model 2, c) Model 3, d) Model 4.

Table 3. Linear gas flow velocity measurements in catalyst beds across different reactor configurations. (highlighted in Fig. 7).

	Model 1	Model 2	Model 3	Model 4
Linear flow velocity (m/s)	V1=0.263	V1=0.161	V1=0.026	V1=0.072
	V2=0.116	V2=0.223	V2=0.070	V2=0.093
	V3=0.157	V3=0.295	V3=0.080	V3=0.112
	V4=0.196	V4=0.230	V4=0.126	V4=0.146
	V5=0.257	V5=0.288	V5=0.173	V5=0.175

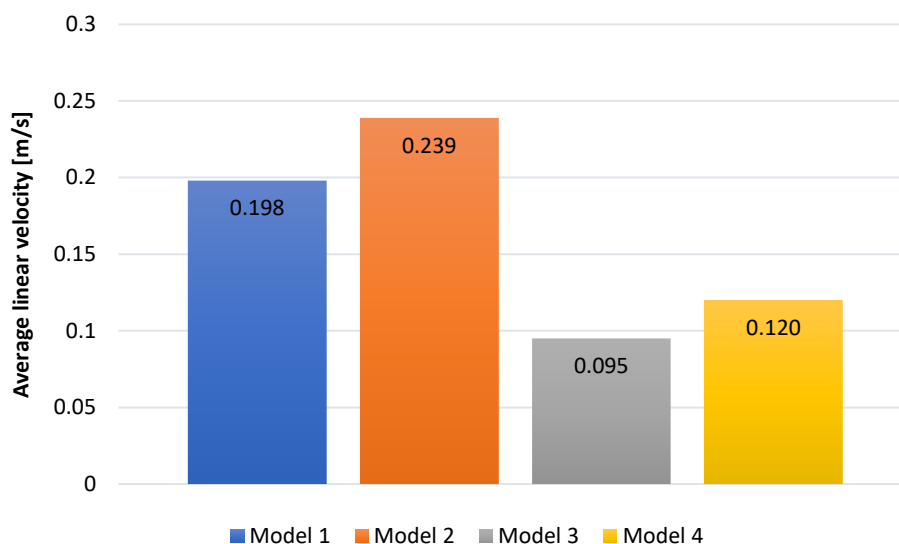


Fig. 8. Average linear gas flow velocity inside the catalysts beds within computational domains, determined for the four catalytic basket models based on CFD simulations.

When comparing the results of linear velocity values for measured fields, Model 2 has the highest measured value of linear velocity. The values obtained for Model 2 are half as high as for Model 4 despite radial flow in both cases. In the case of Model 1 with mixed radial-axial flow, the maximum values of the linear flow velocity obtained are slightly lower than those obtained in Model 2. Model 3 has the lowest values of the linear flow velocity on the catalyst beds using a mixed axial-radial gas flow through the beds. The highest measured value of the linear flow velocity for Models 3 and 4 is the same. However, in Model 3, in almost the entire cross-section, the obtained values of the linear flow velocity are significantly lower than in Model 4. The lowest obtained linear flow velocity for Model 3 is almost 3 times lower than the lowest value obtained for Model 4.

The highest average linear gas flow velocity values inside the catalysts beds were obtained for the variant of catalytic basket represented by Model 2 (two radial catalysts beds installed coaxially along the reactor axis, spatially separated). Radial reactors are characterised by having lower gas flow resistance than axial reactors. Therefore, the average linear gas velocity value for Model 2 was expected to be lower than for Model 1, where the gas distribution in the catalytic beds is in the axial and radial directions. However, CFD simulations results indicated otherwise. In addition, it was found that the average velocity value for Model 2 was twice as high as that determined for Model 4, even though in both models, the gas

flow direction throughout both catalyst beds was radial. However, in the latter case, the beds were arranged coaxially along the reactor diameter and contacted to each other through a porous baffle. It means, that the cross-section of the gas flow field between the catalysts beds in Model 4 did not change. In Model 1, the gas flowed through the first catalyst bed axially without changing the cross-section, and the linear velocity distribution in this bed was uniform. This allowed the gas to flow into the second radial catalyst bed with a lower linear velocity, which resulted in a lower average gas velocity in the whole catalytic area.

The lowest average linear velocity value was obtained for Model 3, characterized by a mixed axial-radial flow in the catalytic zone. In this case, unlike Model 1, the beds of both catalysts contacted each other through a porous baffle and were not spatially separated. In almost the entire cross-section of both catalysts beds, the measured linear gas velocity values for Model 3 were several times lower than those determined for Model 4. It indicates that using a mixed axial-radial flow can improve the efficiency of catalysts by lowering the linear velocity of gases in catalyst beds. However, there is a particular risk of creating dead zones in the first catalyst bed in its upper part, where  $V_{(<V)} \rightarrow 0$  m/s. In these areas, the catalyst layer may not work.

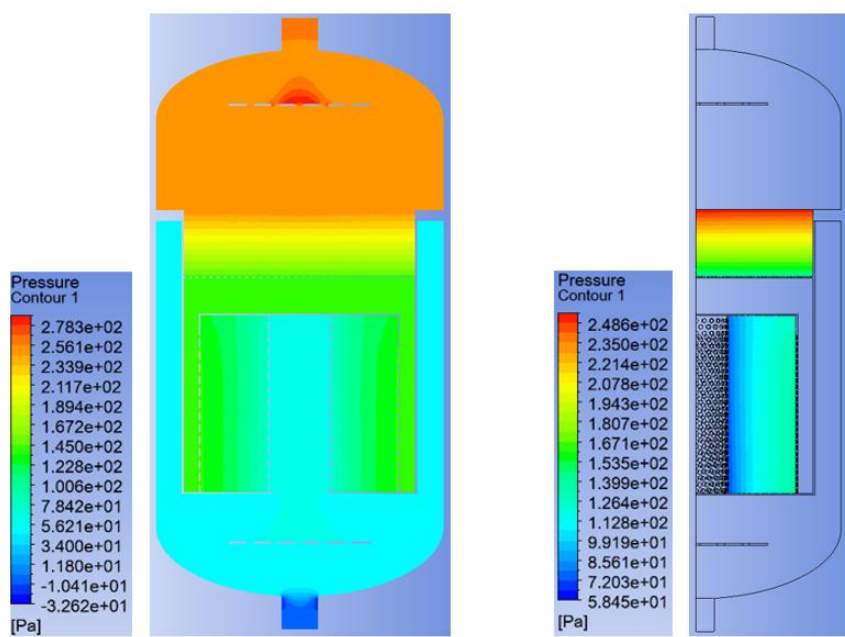
The difference between the smallest (Model 3) and the greatest average value of the linear gas flow velocity was 50.2% (the average value for Model 3 was two times lower than for

Model 2, Table 3). The difference in average linear gas flow velocity values determined for Model 3 and Model 4, in which the catalyst beds contacted each other through a porous baffle, was 20.8%. In contrast, for the variants of the catalytic basket design with axial and radial flow (Model 1 and Model 3), it was as much as 52%. The above results indicate that the velocity value in the dual-bed catalytic basket is influenced by a gas distribution on the catalyst beds (in the radial or axial-radial direction) and their mutual arrangement in the reactor. The results of the CFD method indicate that the catalytic basket

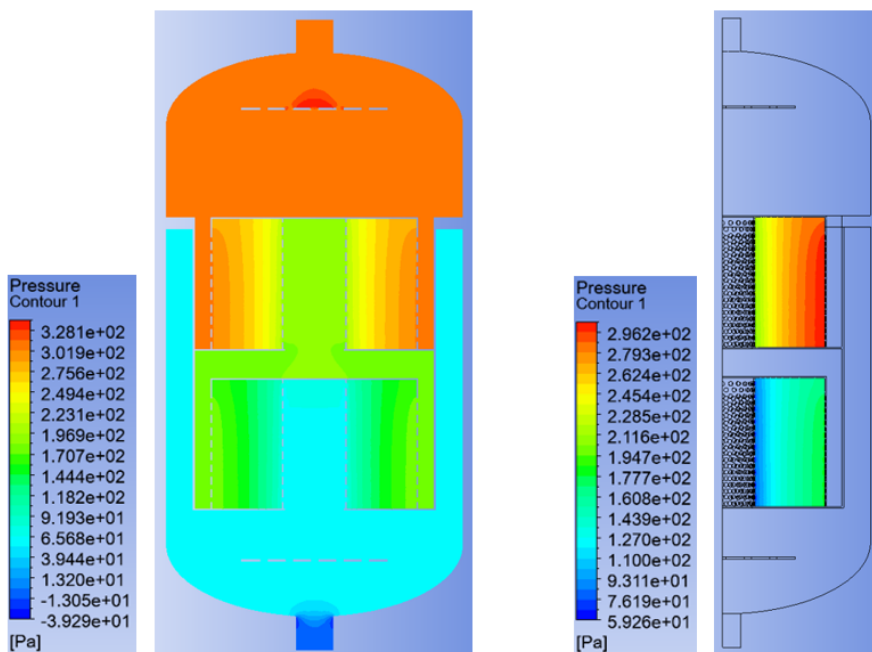
design significantly influences the linear gas flow velocity profile within the catalyst beds. This will increase the removal efficiency of  $\text{NO}_x$  and  $\text{N}_2\text{O}$  and affect the reliability of industrial plants' catalytic processes.

### 3.2. Pressure contour inside the catalytic reactor

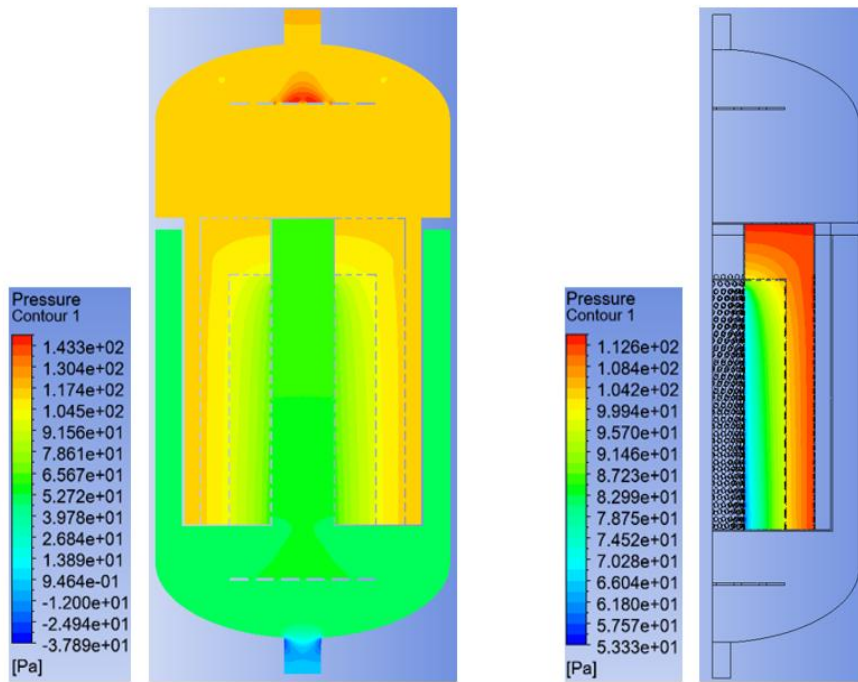
Figure 9 shows the pressure drop contours inside the dual-bed catalytic reactor, obtained based on CFD simulations for the four variants of the catalytic baskets. Table 4 shows the average pressure drop values across the catalyst beds (bed A and bed B).



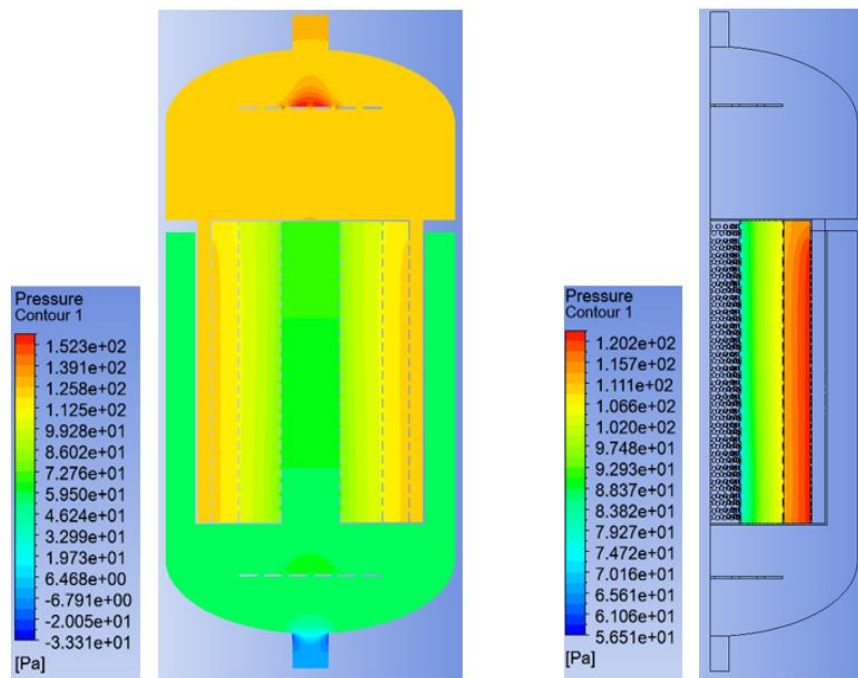
a)



b)



c)



d)

Fig. 9. Contours of gas pressure drop across the catalysts beds inside the computational domains, representing different variants of a dual-bed catalytic reactor: a) Model 1, b) Model 2, c) Model 3, d) Model 4.

Table 4. The average pressure drop values across the catalysts beds (bed A and bed B) for different variants of the dual-bed catalytic reactor.

Pressure drop	Model 1	Model 2	Model 3	Model 4
$\Delta P$ , (Pa)	bed A = 118 bed B = 79	bed A = 120 bed B = 121	bed A = 17 bed B = 53	bed A = 13 bed B = 55

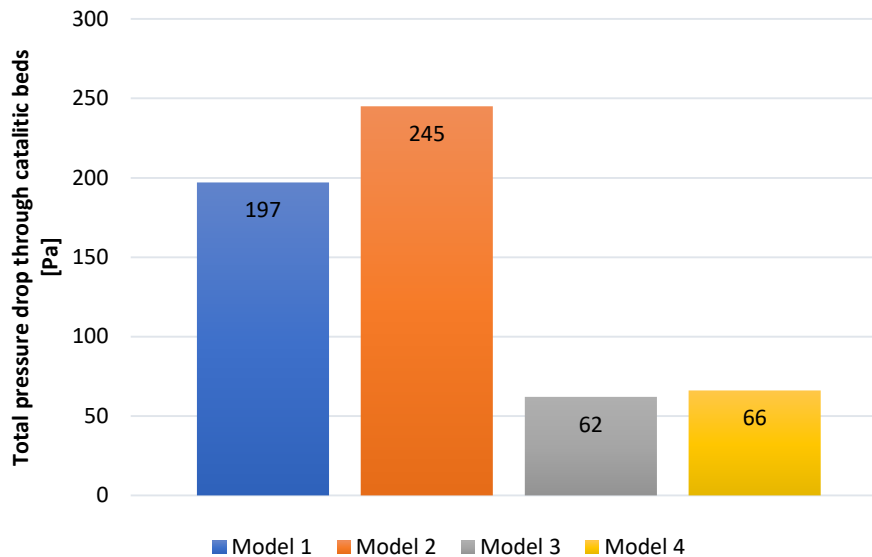


Fig. 10. Total pressure drop values in the dual-bed catalytic reactor for different variants of the catalytic basket design.

The highest gas pressure drops across both catalysts beds were found for Model 2, even though the gas flow direction is radial in both cases. In Model 1, as expected, the gas flow resistance through bed A, in which flow was in the axial direction, was higher than for the radial bed B. The average  $\Delta P$  value determined for bed B in Model 1 was more than 1.5 times lower than for bed B in Model 2, despite the gas flows throughout this bed in the radial direction. These differences in the gas flow resistances throughout both catalytic beds may be related to the significant effect of changes in the cross-sectional area of the flow field in Model 2. In Model 1, gas flows from the inlet zone downstream of the deflector to the bed A zone without changing the discharge's cross-section. For Model 2, the cross-section flow profile upstream of bed A changes (flow through bed A in the radial direction), and the zone of the gas inflow to the catalysts beds is smaller than in other models. This translates into more significant disturbances in the gas flow and pressure drops across the beds. Separating the catalysts beds with a space (Model 1 and Model 2) results in greater gas flow resistances across these beds, than placing them in direct contact and separating only with a porous baffle (Model 3 and Model 4). Then, we deal with a change in the profile of the gas distribution between the beds and more significant turbulence in a gas stream. A problem with installing the catalysts beds in direct contact is the inability to inject a reductant ( $\text{NH}_3$  or  $\text{CH}_4$ ) before bed B. Such variants of the dual-bed catalytic reactor (Model 3 and Model 4) can only be used in the SCR-de $\text{NO}_x$  +

LT-de $\text{N}_2\text{O}$  technology, in which the reducing agent is introduced only upstream of the first catalyst bed [10].

The outcomes demonstrated in Table 4 and Fig. 10 show that the most advantageous design variant of a dual-bed catalytic reactor is represented by Model 3, with axial-radial gas flow through catalysts beds, separated from each other only by a porous baffle. The least advantageous design variant of a dual-bed catalytic reactor is the one represented by Model 2. The difference between the values of total pressure drop determined for Model 2 and Model 3 was 183 Pa. Slight differences in the values of total pressure drop, at the level of 4 Pa, were found between Model 3 and Model 4, in which catalyst beds were separated from each other only by a porous baffle. Model 4 used a basket cover plate with solid side walls to save the system from avoiding the stream in case of formed catalyst settling. In Model 3, the basket cover plate is perforated. That is probably why there are higher gas flow resistances in Model 4 despite the radial gas flow direction throughout both catalysts beds.

### 3.3. Comparison of different dual-bed catalytic reactor variants

The pressure drop across the porous bed is proportional to the length of the gas flow path. The longer it is, the higher the flow resistance will be, assuming a constant volumetric gas flow rate and constant fluid properties/parameters. This applies to both laminar and turbulent flow. According to a constant volumetric gas flow rate, the linear velocity is influenced by the section

flow field (velocity value  $V$  in the porous medium is inversely proportional to the cross-sectional area of the flow field ( $A$ ):  $V = Q/A$  [m/s]). Therefore, by modifying the length of the gas flow path throughout the porous beds and the cross-section of the flow field, it is possible to influence the linear gas velocity and pressure drops across the catalysts beds.

The CFD simulation results indicate, that in the case of installing two catalysts beds in the annular basket compartments, forcing the radial direction of the gas flow throughout these beds, it is more advantageous to arrange them coaxially along the reactor diameter and separate them from each other only by a porous baffle (Model 4). On the other hand, it is disadvantageous to arrange the beds coaxially along the reactor axis and separate them by a space (Model 2). A similar situation occurs in the case of a dual-bed catalytic reactor with axial-radial flow. Separating the two catalysts beds with a space (which can be used to introduce a reducing agent into the purified gas upstream of the second catalytic bed) results in greater turbulence in the gas stream directed to the second catalyst bed, contributes to a change in the cross-section of the flow field and, as a result, to greater linear velocity and pressure drops values. Larger  $\Delta P$  values obtained for the radial flow reactor (represented by Model 4) compared to the axial-radial one (represented by Model 3) may be due to the differences in the design of the catalytic basket cover plate.

The advantage of using mixed axial-radial flow is that it allows the entire catalyst volume to be engaged in the process without gas avoiding the bed caused by the settling catalyst. Additionally, axial-radial flow ensures low-pressure drops. In radial reactors, settling of the catalyst bed as a result of its better packing, thermal shrinkage or abrasion carries the risk of creating gas by-passing zones. Therefore, it is necessary to

provide an excess catalyst volume in relation to the amount required to obtain the desired process efficiency and to use a cover plate with solid side walls in order to seal the bed.

#### 4. Conclusions

The work presents the results of numerical calculations for the four variants of dual-bed catalytic reactor, differing in the way the gas flows throughout two catalysts beds and their mutual arrangement in the reactor. It was found that the construction of the catalytic basket, designed to install two catalysts beds in one reactor, has a significant influence on the linear gas flow velocity and pressure drops across the beds. In order to ensure the lowest possible values of both parameters, it is advantageous to arrange both catalyst beds coaxially next to each other and separate them only with a porous baffle. Separating both catalysts beds with a space contributed to generating turbulence in the gas-distributing to the bed B and changes in the flow field's cross-section. This resulted in an increase in the linear gas velocity in the catalytic section and a greater pressure drop in the reactor. The most advantageous variant is a dual-bed catalytic reactor with mixed axial-radial flow throughout both beds, separated only by a perforated baffle, for which the lowest values of the  $V$  and  $\Delta P$  parameters were obtained. This type of solution can be used, for example, to purify tail gases from nitrogen oxides by a selective catalytic reduction of  $\text{NO}_x$ , low-temperature  $\text{N}_2\text{O}$  decomposition, and other catalytic processes.

The presented research method is limited to using constant gas properties, omitting chemical reactions and using ideal boundary conditions. Nevertheless, the research results provide many valuable clues and contribute to significant progress in the design of dual-bed catalytic reactors.

#### References

1. Greenhouse Gas Protocol, IPCC Global Warming Potential Values, 7.08.2024, <https://www.ipcc.ch/report/ar6/wg1/chapter/chapter-7/#7.6>.
2. Forster P., Ramaswamy V, Artaxo P, Bernsten T, Betts R, Fahey D W, Haywood J, Lean J, Lowe D C, Myhre G, Nganga J, Prinn R, Raga G, Schulz M, Van Dorland R. Changes in Atmospheric Constituents and in Radiative Forcing. Chapter 2. *Environ. Sci.* 2007; 39: 129–234, <http://www.ipcc.ch/pdf/assessment-report/ar4/wg1/ar4-wg1-chapter2.pdf>.
3. Skalska, K, Miller J S, Ledakowicz S. Trends in  $\text{NO}_x$  abatement: A review. *Science of the total environment* 2010; 408(19): 3976-3989, <https://doi.org/10.1016/j.scitotenv.2010.06.001>.
4. Woodrow P. Nitric oxide: Some nursing implications. *Intensive Crit. Care Nurs.* 1997; 13:87–92, [https://doi.org/10.1016/S0964-3397\(97\)80186-3](https://doi.org/10.1016/S0964-3397(97)80186-3).
5. Mainhardt H, Kruger D.  $\text{N}_2\text{O}$  Emissions from Adipic Acid and Nitric Acid Production. *IPCC good practice guidance and uncertainty*

management in national greenhouse gas inventories 2001.

[https://www.ipcc-nggip.iges.or.jp/public/gp/bgp/3\\_2\\_Adipic\\_Acid\\_Nitric\\_Acid\\_Production.pdf](https://www.ipcc-nggip.iges.or.jp/public/gp/bgp/3_2_Adipic_Acid_Nitric_Acid_Production.pdf).

6. Reference Document on Best Available Techniques for the Manufacture of Large Inorganic Chemicals—Ammonia, Acids and Fertilisers 2007, [https://eippcb.jrc.ec.europa.eu/sites/default/files/2019-11/lvic\\_aaf.pdf](https://eippcb.jrc.ec.europa.eu/sites/default/files/2019-11/lvic_aaf.pdf).
7. EU Emission Trading System (EU ETS) 2005, <https://icapcarbonaction.com/en/ets/eu-emissions-trading-system-eu-ets>.
8. Kruczyński S W, Orliński P, Ślęzak M. The comparative analysis of catalytic properties of Group 11 elements in NO<sub>x</sub> reduction by hydrocarbons in the presence of oxygen. *Eksploatacja i Niezawodność* 2022; 24(2), <http://doi.org/10.17531/ein.2022.1.19>.
9. Schwefer M, Groves M, Seifert R, Maurer R. ThyssenKrupp Industrial Solutions, AG. Method and Device for Reducing the NO<sub>x</sub> and N<sub>2</sub>O of Gases. U.S. Patent EP1515791B1, 3 August 2011.
10. Schwefer M, Seifert R, Pinnow S. ThyssenKrupp Industrial Solutions, AG. Device and Method for Eliminating NO<sub>x</sub> and N<sub>2</sub>O. U.S. Patent US20140363359A1, 11 December 2014.
11. Granger J F, Casale S A. Method and Apparatus for Removing NO<sub>x</sub> and N<sub>2</sub>O from a Gas. US Patent US11325069B2, 10 May 2022.
12. Wilk M, Inger M, Prokop U, Franczyk E, Sojka Z, Kotarba A, Adamski A, Stelmachowski P, Piskorz W, Zasada F. Uniwersytet Jagielloński, Instytut Nawozów Sztucznych, Catalyst for low-temperature decomposition of dinitrogen oxide and a process for the preparation thereof, WO2009142520A1, 26 November 2009.
13. Capała P, Ruszak M, Rudawska A, Inger M, Wilk M. The Technology of Tail Gases Purifying in Nitric Acid Plants and Design of deN<sub>2</sub>O and deNO<sub>x</sub> Reactors. *Applied Sciences* 2023; 13(13), 7492, <https://doi.org/10.3390/app13137492>.
14. Perbandt C, Bacher V, Groves M, Schwefer M, Seifert R, Turek T. Kinetics and Reactor Design for N<sub>2</sub>O Decomposition in the EnviNO<sub>x</sub> (R) Process, *ChemieIngenieur Technik* 2013; 85(5):705-709, <https://doi.org/10.1002/cite.201200163>.
15. Ward A M, Chemical Industries PLC, Catalytic Reactor, U.S. Patent WO2001023080A1, 5 April 2001.
16. Tarozzo M, Filippi E, Rizzi E. Casale SA. Wall System for Catalytic Beds of Synthesis Reactors and Relative Manufacturing Process, U.S. Patent EP2014356A1, 14 January 2009.
17. Liu H, Guo T, Yang Y, Lu G. Optimization and Numerical Simulation of the Flow Characteristics in SCR System. *Energy Procedia* 2012; 17, 801–812, <https://doi.org/10.1016/j.egypro.2012.02.173>.
18. Gao Y, Liu Q, Bian L. Numerical Simulation and Optimization of Flow Field in the SCR Denitrification System on a 600 MW Capacity Units. *Energy Procedia* 2012; 14, 370–375, <https://doi.org/10.1016/j.egypro.2011.12.944>.
19. Hong W P, Jian S C. Numerical Simulation of Flue Gas Flow and NH<sub>3</sub> Diffusion Properties in SCR System. *Adv. Mater. Res.* 2014; 881–883, 1819–1822, <https://doi.org/10.4028/www.scientific.net/AMR.881-883.1819>.
20. Baker M J. CFD simulation of flow through packed beds using the finite volume technique. University of Exeter, United Kingdom, ProQuest Dissertations & Theses: 2011.
21. Mi J, Pitsko D A, Haskew T. CFD Applications on Selective Catalytic NO<sub>x</sub> Reduction (SCR) Systems. In Fluids Engineering Division Summer Meeting 2003; 36967, 2139-2146, <https://doi.org/10.1115/FEDSM2003-45436>.
22. Mi J. CFD for SCR design. *Southern Company Inc., Atlanta* 2004.
23. Rogers K, Albrecht M, Varner M. Numerical modeling for design optimization of SCR applications. *ICAC NO<sub>x</sub> Forum*. Washington: ICAC, 2000.
24. Ranade V V. Fixed bed and other types of reactors. *Computational Flow Modeling for Chemical Reactor Engineering*; Elsevier. Amsterdam, The Netherlands, 2002:403-423. [https://doi.org/10.1016/S1874-5970\(02\)80014-5](https://doi.org/10.1016/S1874-5970(02)80014-5)
25. Ye X. Research and Application of Multi-dimension Numerical Simulation Optimization for SCR DeNO<sub>x</sub> Flow Field. *IOP Conference Series: Earth and Environmental Science* 2018; 113:1, doi :10.1088/1755-1315/113/1/012181.
26. Kruczyński S, Ślęzak M. A simulation and experimental verification of the operation of the oxidising catalytic converter in diesel engine. *Maintenance & Reliability/Eksploatacja i Niezawodność* 2024; 26:2, <http://doi.org/10.17531/ein/184090>.
27. Ahmadi S, Sefidvash F. Study of Pressure Drop in Fixed Bed Reactor Using a Computational Fluid Dynamics (CFD) Code. *ChemEngineering* 2018; 2:14, <https://doi.org/10.3390/chemengineering2020014>.
28. Sun W, Ye M, Gao Y, Sun Y, Qian F, Lu J, Wu S, Huang N, Xu B. Effect of Catalyst Inlet Flow Field Distribution Characteristics on Outlet NO Concentration Distribution in SCR Denitration Reactor Based on Monte Carlo Method. *Atmosphere* 2022; 13:931,

<https://doi.org/10.3390/atmos13060931>.

29. Wang H, Sun J, Li Y, Cao Z. Numerical Simulation and Optimization of SCR-DeNO<sub>x</sub> Systems for Coal-Fired Power Plants Based on a CFD Method. *Processes* 2022; 11(1):41, <https://doi.org/10.3390/pr11010041>.
30. Ye M, Qian F, Gao Y, Lu J, Han Y, Huang N, Xu B, Wu H. CFD analysis of influencing factors on SCR denitration efficiency of sintering flue gas based on response surface methodology. *Atmospheric Pollution Research* 2021; 12:101107, <https://doi.org/10.1016/j.apr.2021.101107>.
31. Ye D, Wang X, Wang R, Gao S, Liu H, Wang H. Optimizing flow field in an SCR system of a 600 MW power plant: Effects of static mixer alignment style. *Waste Disposal and Sustainable Energy* 2021; 3:339–346, <https://doi.org/10.1007/s42768-021-00082-z>.
32. Vandewalle L A, De S, Van Geem K M, Marin G B, Bos R. Reactor Engineering Aspects of the Lateral Flow Reactor. *Industrial & Engineering Chemistry Research* 2020; 59:11157–11169, <https://doi.org/10.1021/acs.iecr.0c01229>.
33. Preller A C N. Numerical modelling of flow through packed beds of uniform spheres. Doctoral dissertation, North-West University, 2011.
34. Rizzi, E.; Casale SA. Axial-Radial Flow Catalytic Chemical Reactor with Two Layers of Catalyst. U.S. Patent US10596538, 24 March 2020.